Cellulose (2020) 27:3611–3622
https://doi.org/10.1007/s10570-020-03027-7

ORIGINAL RESEARCH

Interaction of nitrocellulose with pentaacyloxyphenyl fullerene derivatives: autocatalytic inhibition in thermal decomposition of nitrocellulose

Yang Zhao · Bo Jin · Rufang Peng · Ling Ding

Received: 25 November 2019 / Accepted: 26 January 2020 / Published online: 8 February 2020

Abstract The safe storage of nitrocellulose has become challenging due to their requirements of extreme storage environments, and existing stabilizers cannot fully meet the demand. Thus, developing new high-performance stabilizers to improve the stability of nitrocellulose is urgently needed. Considering the stabilizing mechanism of stabilizers and the excellent free radical scavenging ability of fullerenes, two novel fullerene-based stabilizers, pentaacyloxyphenyl fullerene derivatives (PAOP-C_{60}), were designed and synthesized, and their structures were characterized by FTIR, UV–Vis and NMR. The thermal action of PAOP-C_{60} during thermal decomposition process of nitrocellulose was studied by thermal analysis, which indicating that the thermal stability of nitrocellulose was increased with addition of PAOP-C_{60} and the PAOP-C_{60} was found to exhibit superior thermal stability than traditional stabilizer. The results of electron spin resonance showed that fullerene-based stabilizers had a significant scavenging effect on nitrogen oxide radicals, and the IC50 of PAOP-C_{60} (0.674–0.818 g L^{-1}) was smaller than that of diphenylamine (1.717 g L^{-1}). Moreover, the intermediate product produced by PAOP-C_{60} and nitrocellulose action was extracted and characterized by FTIR. A possible stabilization mechanism of PAOP-C_{60}, which was different from traditional stabilization mechanism, was proposed.

Keywords Nitrocellulose · Fullerene derivative · Stabilizer · Radical scavenger · Thermal analysis

Y. Zhao · B. Jin (✉) · R. Peng (✉) · L. Ding
State Key Laboratory of Environment-friendly Energy Materials, Southwest University of Science and Technology, Mianyang 621010, Sichuan, China
e-mail: jinbo0428@163.com

R. Peng
e-mail: rfpeng2006@163.com

Introduction

Nitrocellulose, as a famous energetic polymer, has been widely used in propellants and weapon systems. However, the fracture of the fragile nitrate bond (CH_2–O–NO_2) in the nitrocellulose structure generates a large amount of nitroxide radicals, which accelerate the decomposition of nitrocellulose and give rise eventually to self-heating and safety hazards (Wang et al. 2017; Heil et al. 2017; Luo et al. 2019a; Merzhanov and Abramov 2010; Ossa et al. 2011; Saunders and Taylor 1990; Kubota 2010; Tsang and Herron 1991; Wiegand et al. 1990). The safe storage of nitrocellulose has become challenging due to its inflammable and autocatalytic thermal decomposed characteristics, developing suitable methods for autocatalytic inhibition is urgently needed to save manpower and material resources (He et al. 2017; Hussien et al. 2018; Jain et al. 2016). Adding stabilizers to nitrocellulose during long-term storage

can significantly improve the thermal stability of nitrocellulose without changing its inherent properties and save economic cost.

The conventional stabilizers such as diphenylamine (DPA), 2-nitrodiphenylamine (2-NDPA), *p*-nitro-*N*-ethylaniline, *N*,*N*′-diethyl-*N*,*N*′-diphenylurea (C1), *N*,*N*′-dimethyl-*N*,*N*′-diphenylurea (C2), and *N*-methyl-*N*′,*N*′-diphenylurea (AKII) are alkaline compounds. These alkaline substances act as stabilizers by reacting with acid intermediates produced by the thermal decomposition of nitrocellulose (Lindblom 2002; Trache and Tarchoun 2018). However, the strong alkalinity of aromatic amines give it the ability of combined with nitrogen oxides, which can inhibit the autocatalytic decomposition of nitrocellulose, but also lead to unexpected saponification reaction (Purves et al. 1950; Klerk and Wim 2015; Katoh et al. 2010; Drzyzga 2003). While urea derivatives are weak in alkalinity but resulting in unsatisfactory stability and have a bad compatibility with nitrocellulose (Fryš et al. 2011; Hassan and Shehata 2010; Wilker et al. 2007). Obviously, the alkalinity of stability limits the stabilizing effect of stabilizer and the thermal stability of nitrocellulose. Therefore, the design of new types of stabilizers is the focus of the safe storage of nitrocellulose at present, lots of novel stabilizers have been synthesized.

In 2016, several novel stabilizers without amine moiety were designed and synthesized (Krumlinde et al. 2016), these stabilizers provide a new strategy of design and synthesize novel stabilizers, aromatic compounds containing carbonyl oxygen. However, these stabilizers don't improve thermal stability of nitrocellulose in the high temperature, and there is no change in the stabilization mechanism.

Our previous work noted the potential application of fullerene as an efficient free radical scavenger in the stabilizers. In consideration of the structural characteristics of these stabilizers and the special free radical scavenging function of fullerenes (Gharbi et al. 2005; Krusic et al. 1991; Taylor and Walton 1993), novel pentaacyloxyphenyl fullerene derivatives were designed and synthesized by Friedel–Crafts alkylation using hexachlorofullerene as precursor. Considering the currently reported stabilizers, DPA is one of the state-of-the art stabilizers, which has the advantage of low price and wide application (Krumlinde et al. 2016). Herein, we first studied the thermal stability and compatibility of these pentaacyloxyphenyl fullerene derivatives (PAOP-C_{60}), and it found to exhibit superior thermal stability than traditional stabilizer DPA. The reaction of these fullerene-based stabilizers in the thermal decomposition of nitrocellulose was studied by thermal analysis and ESR, and the intermediate products produced by the interaction of PAOP-C_{60} and nitrocellulose was characterized via FTIR. Therefore, a corresponding stabilization mechanism was proposed.

Experimental section

Synthesis of pentaacyloxyphenyl fullerene derivatives

Hexachlorofullerene $C_{60}Cl_6$ (46 mg, 0.05 mmol) was completely dissolved in nitrobenzene (20 mL), then phenyl formate (1.83 g, 15 mmol) or phenyl acetate (2.04 g, 15 mmol) was added, followed by $TiCl_4$ (0.95 g, 5 mmol) as catalyst. The mixed solution was stirred at 100 °C until TLC showed that $C_{60}Cl_6$ was completely consumed and the mixed solution changed from orange to dark brown. After work up, the excess catalyst and solvent were removed to obtain red-brown crude products. The pentaacyloxyphenyl fullerene derivatives were purified by column chromatography (silica gel). Elution was performed with carbon disulfide-ethyl acetate (1/1) for 2a and carbon disulfide-ethyl acetate (3/1) for 2b. The process is shown in Fig. 1.

2a. ^{1}H NMR (d^6-DMSO, 600 MHz): 9.67 (s, 2H), 9.65 (s, 2H), 9.55(s, 1H), 7.69 (d, J = 8.64 Hz, 4H), 7.46 (d, J = 8.64 Hz, 4H), 6.99 (d, J = 8.76 Hz, 2H), 6.77 (t, J = 6.78 Hz, 8H), 6.51 (d, J = 8.76 Hz, 2H), 5.76 (s, H-C_{60}, 1H). ^{13}C NMR (d^6-DMSO, 150 MHz): 167.42 (–HCO), 157.65, 157.52, 157.29, 155.61, 152.39, 150.19, 148.52, 148.47, 148.15, 148.86, 147.84, 147.80, 147.60, 147.27, 147.01, 146.94, 146.77, 146.73, 146.59, 145.94, 145.60, 145.43, 145.33, 144.56, 144.36, 144.14, 143.94, 132.16 (sp^2), 131.98 (sp^2), 131.20 (sp^2), 129.13 (sp^2), 129.08 (sp^2), 128.31 (sp^2), 127.81 (sp^2), 125.94 (sp^2). 116.16 (sp^2), 116.11 (sp^2), 65.55 (sp^3 fullerene cage), 62.10 (sp^3 fullerene cage), 60.03 (sp^3 fullerene cage), 57.90 (sp^3 fullerene cage). FT-IR (KBr, cm^{-1}): 594, 1047, 1208, 1457, 1632, 1746, 2727, 2854, 2919, 2970. UV–Vis (nm): 264.

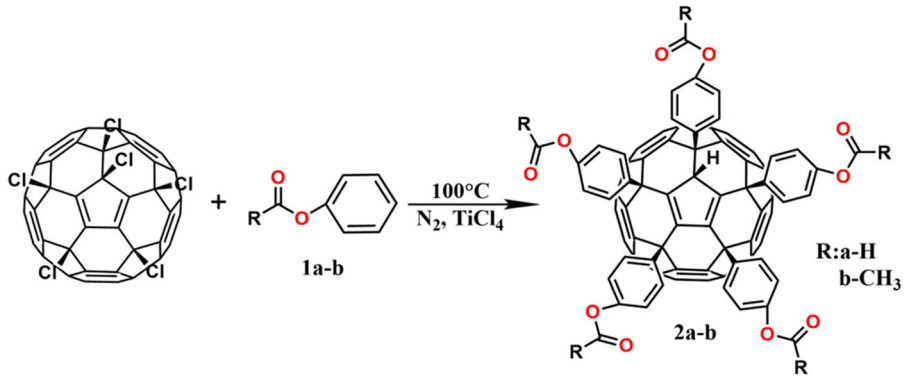

Fig. 1 Synthesis of pentaacyloxyphenyl fullerene derivatives

2b. ^{1}H NMR (d^{6}-DMSO, 600 MHz): 7.68 (t, J = 8.52 Hz, 4H), 7.46 (t, J = 8.52 Hz, 4H), 6.99 (d, J = 8.52 Hz, 2H), 6.77 (t, J = 7.92 Hz, 8H), 6.51 (d, J = 8.52 Hz, 2H), 5.76 (s, H-C_{60}, 1H), 2.28 (s, 12H), 1.99 (s, 3H). ^{13}C NMR (d^{6}-DMSO, 600 MHz): 170.83 (–CO–), 170.80 (–CO–), 157.55, 157.53, 157.09, 153.86, 151.64, 150.91, 150.18, 148.59, 148.39, 148.38, 148.25, 148.08, 147.95, 147.66, 147.24, 147.16, 147.12, 147.08, 145.50, 144.30, 144.09, 144.01, 143.95, 143.85, 143.80, 143.66, 142.66, 137.03 (sp^2), 134.62 (sp^2), 131.25 (sp^2), 129.79 (sp^2), 129.56 (sp^2), 128.58 (sp^2), 126.97 (sp^2), 116.13 (sp^2), 116.11 (sp^2), 115.14 (sp^2), 77.35 (sp^3 fullerene cage), 62.86 (sp^3 fullerene cage), 60.23 (sp^3 fullerene cage), 57.43 (sp^3 fullerene cage), 22.57 (–CH_3), 21.24 (–CH_3). FT-IR (KBr, cm^{-1}): 576, 1052, 1267, 1385, 1462, 1632, 1720, 2853, 2926, 2978. UV–Vis (nm): 263.

Characterization

All organic reagents used were pure commercial products from Aladdin. The solvents were purchased from Chengdu Kelong Chemical Reagents Co. CS_2 was distilled prior to use. Fullerene (99.9%) was purchased from Puyang Yongxin Fullerene Technology Co., Ltd. Silica gels (300–400 mesh) were purchased from Qingdao Hailang Chemical Reagents Co. Nuclear magnetic resonance (NMR) spectra were recorded on a Bruker Avance III 600 spectrometer. $CDCl_3$ was used as solvent and TMS as the internal standard. Fourier transform infrared (FTIR) spectra were obtained from a Nicolet 380 FTIR spectrophotometer (Thermo Fisher Nicolet, USA) with a resolution of 4 cm^{-1} from 400 cm^{-1}. A double-beam light source from 190 nm to 1100 nm was used in the ultraviolet–visible (UV–Vis) spectrophotometer (Thermo Scientific Evolution 201, USA).

Analysis and detection

Methyl violet test was conducted by GJB 770B-2005 method, and the temperature was kept at 134.5 °C. Vacuum stability test (VST) was tested at 90 °C for 48 h with a sample mass of 300 mg. A WCR-1B instrument under air atmosphere at a heating rate of 10 °C min^{-1} was used for differential thermal analysis (DTA). Thermogravimetric (TG) analysis was conducted on an America SDT Q600 synchronous thermal analyzer under air atmosphere at a constant temperature of 134.5 °C with sample masses of 3.0 ± 0.2 mg. A NETZSCH instrument was used in the accelerating rate calorimeter (ARC). Hastelloy bomb with a thermocouple clip located on the bottom of the bomb was used. The procedure for heating–searching–waiting mode was as follows. The heating rate was 10 °C min^{-1}, and the searching time was 30 min. The ESR spectrometer was recorded on a Bruker EMXmicro instrument, and the settings were as follows: microwave power, 2 mW; modulation frequency, 100 kHz; field center, 3440 G; sweep width, 100 G; conversion time, 40.04 ms; time constant, 40.96 s; number of scans, 3; and sweep time, 60.06 s. The amount of detected NO· was determined from the calibration curve for integral intensity of the ESR signal of NO–Fe^{2+}(DETC)$_2$.(-Morley and Keefer 1993).

Results and discussion

Characterization of PAOP-C_{60}

The structure of PAOP-C_{60} was characterized by ^{1}H NMR, ^{13}C NMR, FTIR, and UV–Vis. The structure of products was confirmed by FTIR and UV–vis spectra. The FTIR spectrum of 2a and 2b (Fig. 2a) showed carbonyl absorptions at 1745–1715 cm^{-1}, benzene skeleton vibration absorptions at 160–1450 cm^{-1}, and ester absorptions at 1210–1100 cm^{-1}. Formyl absorption at 2727 cm^{-1} was also found in the FTIR spectra of 2a. UV–vis spectra (Fig. 2b) showed that the characteristic absorption peaks of C_{60} (Hare et al. 2013) and $C_{60}Cl_6$ (Birkett et al. 1993) disappeared, and the blue shift of absorption peaks of 2a and 2b was possibly due to the disappearance of auxochrome.

The characterization of 2a and 2b by NMR (Figs. 3, 4) spectroscopy verified the structure of products. The ^{1}H NMR spectrum of 2a (Fig. 3a) showed five sets of signals with integrals of 2:2:1:4:1, two doublets at δ = 7.65, 7.46 ppm with J = 8.64 Hz, and one triplet at δ = 6.77 ppm with J = 6.78 Hz. The protons on two sets of phenyl were arranged symmetrically around the central cyclopentadiene of the fullerene. The other protons of phenyl on the top of cyclopentadiene exhibited two doublets at δ = 6.99, 6.51 ppm with J = 8.76 Hz. The signals from the aromatic moiety, a singlet for the fullereneyl proton (Krusic et al. 1991) at δ = 5.76 ppm and three singlets for the formyl proton at δ = 9.67, 9.65, 9.55 ppm with integrals of 2:2:1, were observed. This observation revealed that five phenyl formate groups (para) were around the central cyclopentadienyl unit, and the hydrogen atom was at the top of the cyclopentadienyl unit (Birkett et al. 1997). Similarly, the ^{1}H NMR spectrum of 2b (Fig. 4a) showed five sets of signals with integrals of 2:2:1:4:1, a singlet for the fullereneyl proton at δ = 5.76 ppm, and two singlets for the methyl proton at δ = 2.28, 1.99 ppm with integrals of 4:1. The ^{13}C NMR spectra of 2a (Fig. 3b) and 2b (Fig. 4b) clearly established the existence of a plane of symmetry, with 27 signals observed for $sp^{2.86}$ carbons (158–143 ppm). Ten signals (137–115 ppm) were observed for the sp^{2}-carbon atoms of phenyls. The sp^{3}-carbon atoms of the fullerene skeleton were observed at δ = 66–57 ppm for 2a and δ = 78–57 ppm for 2b. One peak at δ = 167.42 ppm for the formyl carbon atom of 2a, two peaks at δ = 170.83, 170.80 ppm for the carbonyl carbon atoms, and two peaks at δ = 22.57, 21.24 ppm for the methyl carbon atoms of 2b were observed.

Nevertheless, all our attempts to obtain a mass spectrum failed presumably due to the decomposition of this complex molecule under electrospray ionization conditions.

The superior molecular structure of these products is as follow: all five organic addends are attached to one hemisphere of the fullerene molecule around a central pentagon unit. This structure has the advantage of retaining the original carbon cage structure of fullerene without destroying the chemical characteristics of fullerene.

Stability performance of PAOP-C_{60}

The chemical compatibility of the PAOP-C_{60} with nitrocellulose is an important index to evaluate whether it could be stored stably for a long time. In general, the difference between the thermal decomposition peak of mixture (1/1) and the one

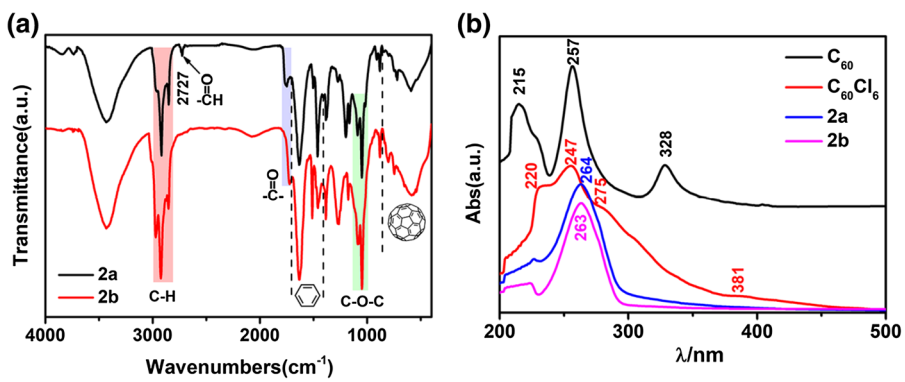

Fig. 2 FTIR (**a**) and UV–Vis (**b**) spectra of 2a and 2b

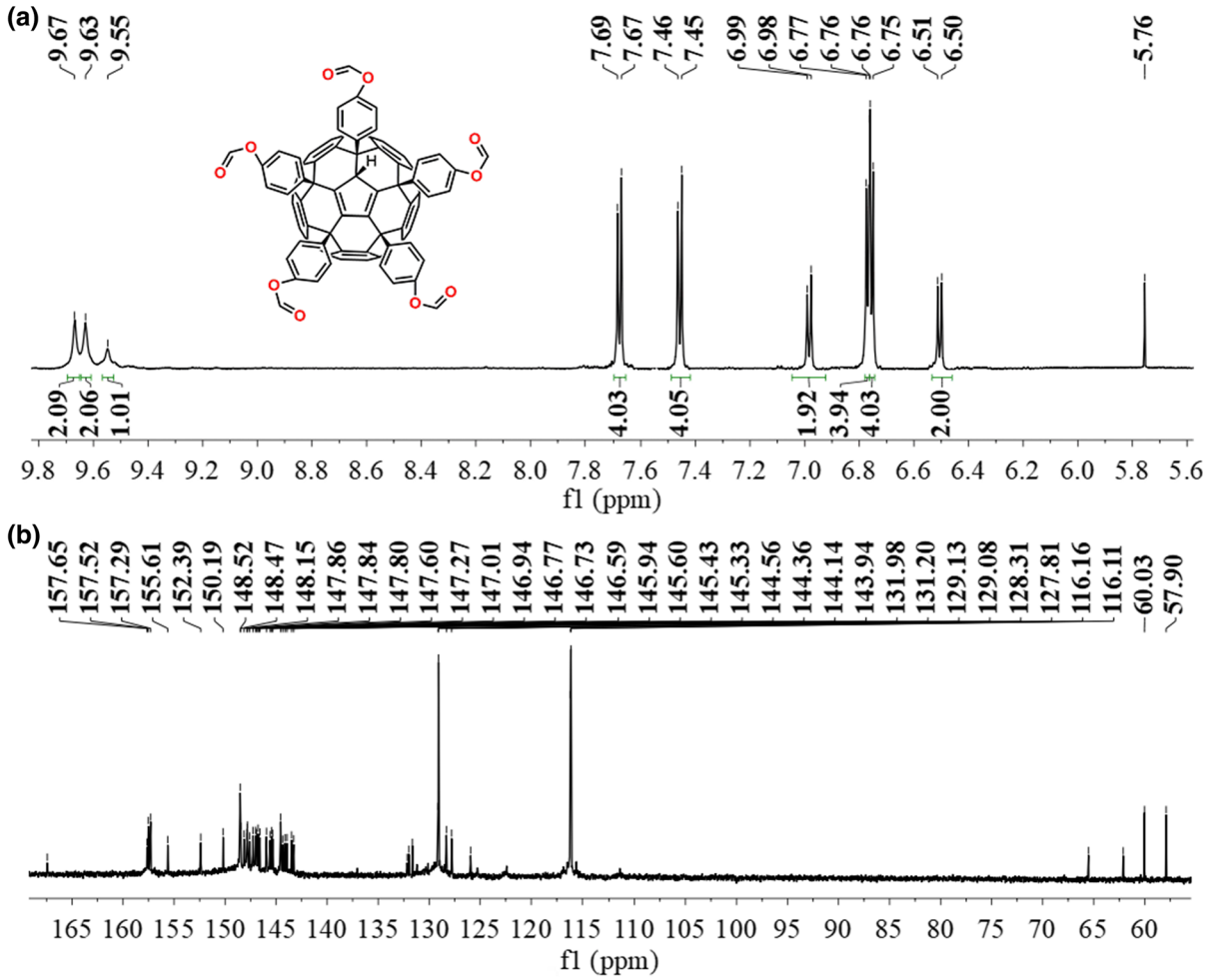

Fig. 3 ^{1}H NMR (**a**), ^{13}C NMR (**b**) spectra of 2a

decomposed at a lower temperature should not exceed 2 C (Defence 2005). The DTA curves of nitrocellulose and PAOP-C_{60} are shown in Fig. 5. The decomposition temperatures of nitrocellulose, 2a, and 2b were 200 °C, 201.49 °C, and 201.92 °C, respectively. The result show that pentaacyloxyphenyl fullerene derivatives have good compatibility with nitrocellulose.

Nitrocellulose sample and three nitrocellulose samples containing 3% (w/w) DPA, 2a, and 2b (S-1: DPA/NC; S-2: 2a/NC; S-3: 2b/NC) were subsequently tested for vacuum stabilities (Luo et al. 2019b) at 90 °C for 48 h. The results are shown in Fig. 6. The amount of gas produced from nitrocellulose samples under the same conditions is usually considered a standard in stability evaluation. The small gas volume leads to good stability. The gas volume per unit mass of the samples were 4.67, 2.79, 0.99, and 0.74 mL g^{-1}. Result showed that 2a and 2b can effectively reduce the amount of gas produced by thermal decomposition of nitrocellulose, and the stability of 2a and 2b are better than that of traditional stabilizer DPA.

The stability of nitrocellulose samples was determined by measuring the time required for the methyl violet paper to change from purple to orange. The time required for nitrocellulose, S-1, S-2, and S-3 in the methyl violet test at 134.5 °C is shown in Table 1. The discoloration time of NC, S-1, S-2, and S-3 was 58, 75, 135, and 160 min, respectively, which indicated that 2a and 2b could effectively prolong the discoloration time. Pentaacyloxyphenyl fullerene derivatives performed better than the traditional stabilizer DPA.

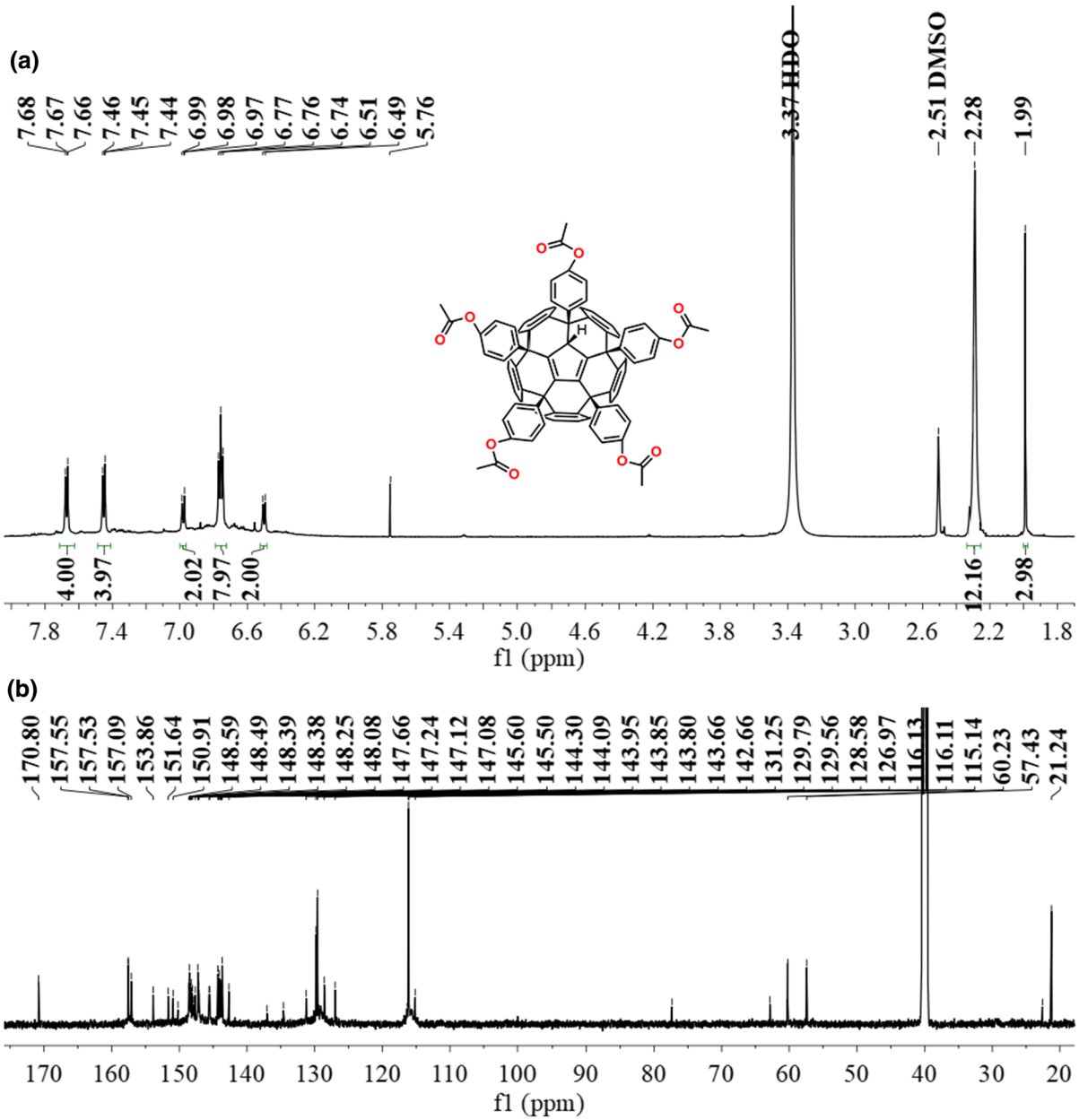

Fig. 4 ^{1}H NMR (**a**), ^{13}C NMR (**b**) spectra of 2b

The isothermal TG of nitrocellulose samples containing different stabilizers was tested in accordance with the previous method (Tang et al. 2016). The stability of nitrocellulose sample is indicated by the weight loss in the same time at the constant temperature. The isothermal TG curves of nitrocellulose, S-1, S-2, and S-3 at 134.5 °C are shown in Fig. 7. S-2 and S-3 had lower weightlessness than nitrocellulose and S-1 within the same time. We took the time with 1% mass loss of samples as a reference to evaluate the stability of stabilizers. The times for nitrocellulose, S-1, S-2, and S-3 were 7.29, 14.11, 21.15, and 22.92 min, respectively. Therefore, the stability of 2a and 2b was superior to that of the traditional stabilizer DPA. The result is highly consistent with those of VST and methyl violet paper method.

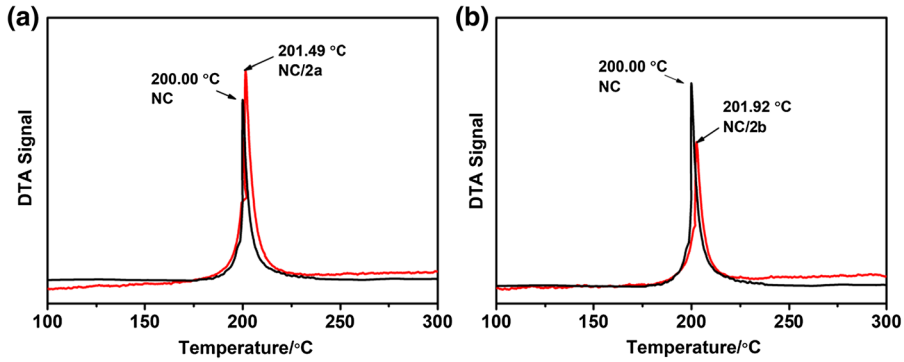

Fig. 5 DTA curve of nitrocellulose and PAOP-C_{60}

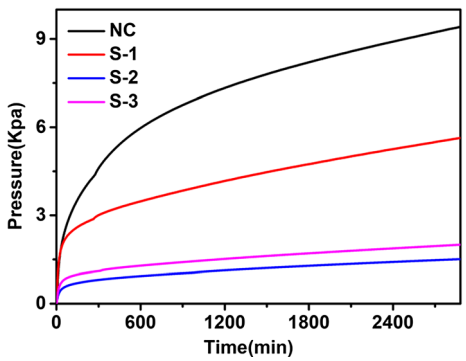

Fig. 6 VST test of NC and S-1-S-3 at 90 °C

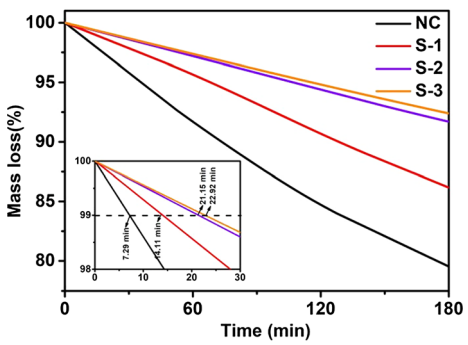

Fig. 7 Isothermal TG curves of NC and S-1-S-3

Table 1 Discoloration time of methyl violet paper test at 134.5 °C

Samples	Stabilizers	Time (min)	Storage for 5 h
NC	–	58	Non-burning and non-exploding
S-1	DPA	75	
S-2	2a	135	
S-3	2b	160	

ARC is an effective tool for the hazard evaluation of energetic materials (Bhattacharya 2005; Dong et al. 2003). This tool can explain the interaction among different components of the sample itself, because the test process is kept in an adiabatic state. The interaction between fullerene derivatives and nitrocellulose was studied by ARC. The results are shown in Fig. 8, and the experimental conditions are listed in Table 2. All the dHR-T curves of nitrocellulose samples have an inflexion, which changes from a lower temperature rising rate to a higher temperature rising rate. The inflexion is regarded as self-accelerating decomposition temperature (T_{SADT}). T_{SADT} is consistent with the stability of nitrocellulose samples. The PAOP-C_{60} can make T_{SADT} move to a high temperature and effectively reduces the highest temperature increase rate.

The ARC data can be used to calculate the time to maximum rate (TMR), which describes the time required for the nitrocellulose samples to decompose thermally from a certain temperature to the maximum rate of thermal decomposition. The safety of nitrocellulose samples and the possibility of chain decomposition can be evaluated.

For n-order decomposition reaction, TMR is defined as follow:

$$\mathrm{TMR} = t_m - t = \int_T^{T_m} \frac{dt}{k\left(\frac{T_f - T}{\Delta T_d}\right)\Delta T_d C_0^{n-1}}$$

where t_m is the time of maximum rate, min; t is the time of initiation decomposition, min; k is the reaction rate constant; T_f is the terminal temperature of exothermic, °C; T is the initiation temperature of

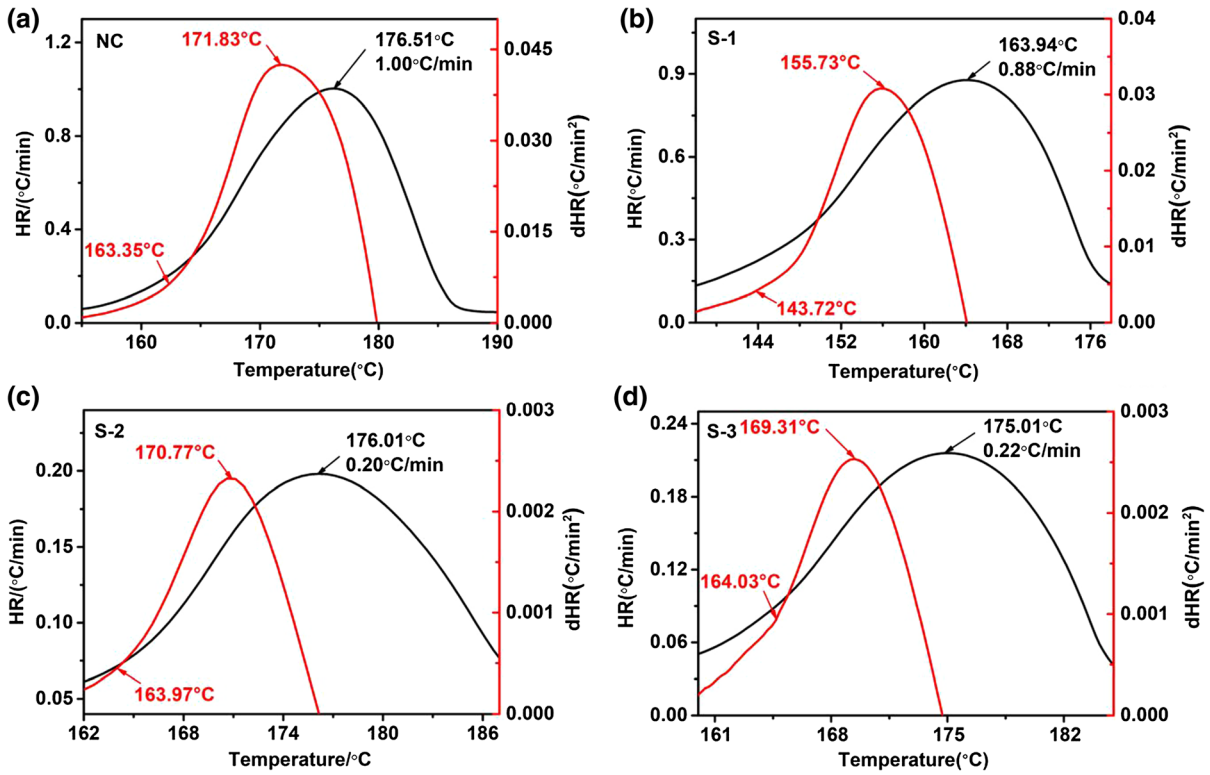

Fig. 8 Heat rate-temperature and self-acceleration rate-temperature curves of nitrocellulose, S-2 and S-3

Table 2 The ARC test results of NC and S-1-S-3

Sample	Stabilizer	Mass (g)	T_{SADT} (°C)	T_m (°C)	HR_m (°C min^{-1})
NC	None	0.08	163.35	176.51	1.00
S-1	DPA	0.08	143.72	163.94	0.88
S-2	2a	0.08	163.97	176.01	0.20
S-3	2b	0.08	164.03	175.61	0.22

exothermic, °C; ΔT_d is the temperature-rising rate, °C min^{-1}; n is the order of reaction; and c_0 is the initiation concentration of samples, mol L^{-1}.

The ARC curves obtained do not contain the terminal of thermal decomposition, because the heat release rate of nitrocellulose samples under adiabatic conditions is relatively slow. For the convenience of calculation, the approximate formula is derived mathematically as follows (Dong et al. 2003):

$$TMR = \frac{RT^2}{m_T E} - \frac{RT_m^2}{m_m E}$$

where HR_T is the temperature-rising rate at T, °C min^{-1}; m_m is the maximum rate, °C min^{-1}; and T_m is the temperature of maximum rate, °C.

The TMR of nitrocellulose samples were calculated to be 278.7, 499.4, 1698.3, and 1726.2 min. The three stabilizers reduced the maximum temperature-rising rates of nitrocellulose from 1.00–0.88, 0.22, and 0.20 °C min^{-1}. The rate and degree of thermal decomposition of nitrocellulose samples showed that the thermal stability of nitrocellulose can be improved greatly by stabilizers, and the PAOP-C_{60} are superior to DPA.

Stabilization mechanism of PAOP-C_{60}

Numerous studies (Morley and Keefer 1993; Hare et al. 2013) have confirmed that the main cause of the poor thermal stability of nitrocellulose is the release of

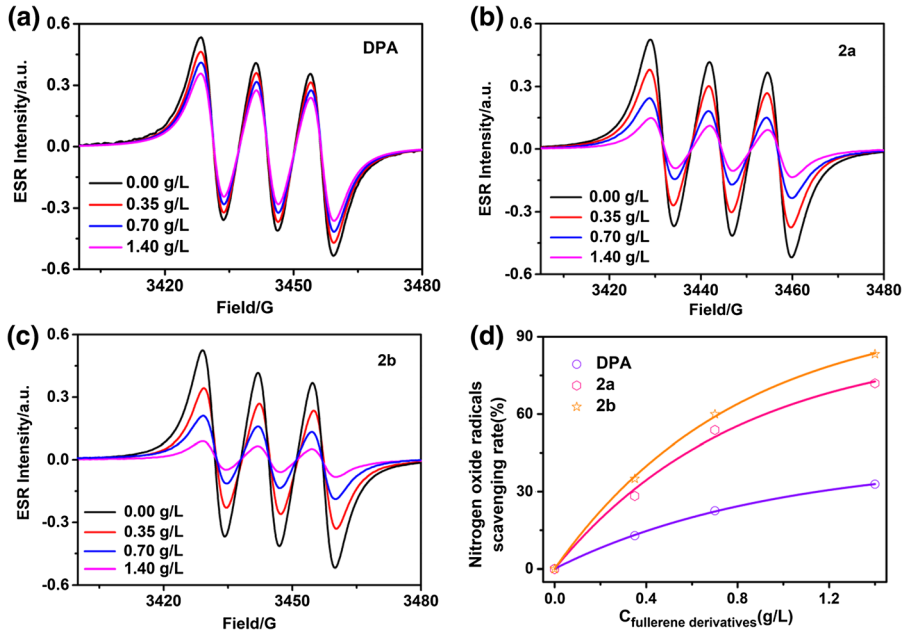

Fig. 9 ESR curves of nitrogen oxide radical scavenging of DPA (**a**), 2a (**b**) and 2b (**c**) with different concentrations, and nitrogen oxide radical scavenging rates (**d**)

nitrogen oxide radicals and other active substances. Therefore, one of the important indicators of stabilization is the nitrogen oxide radical-scavenging efficiency.

We investigated the nitrogen oxide radical-scavenging activity of 2a and 2b in different concentrations (0.00, 0.35, 0.70, and 1.40 g L^{-1}) by electron spin ESR and use DPA as reference, the results are shown in Fig. 9a–c. With increasing the concentration of stabilizers, the ESR signal of nitrogen oxide radicals decreased, thereby showing that all these stabilizers could effectively scavenge nitrogen oxide radicals. The nitrogen oxide radical-scavenging rates of DPA, 2a and 2b were 31.04%, 73.02% and 84.69%, respectively. The results showed that radical-scavenging ability of the stabilizers was consistent with the order of stability, and the radical-scavenging ability of PAOP-C_{60} was stronger than that of DPA. The ability of those pentaacyloxyphenyl fullerene derivatives to scavenge nitrogen oxide radicals may be due to that the carbon sphere of fullerene fits well into the active site of free radicals (Gharbi et al. 2005; Krusic et al. 1991; Taylor and Walton 1993), which allows the reactivity of fullerene to react with free radicals.

From Fig. 9d, the fitting curves of nitrogen oxide radical-scavenging rates of different concentrations of 2a and 2b can be expressed as follows:

$$\eta = a \times \left(1 - b^{C}\right)$$

where C denotes the concentrations of DPA, 2a and 2b in g L^{-1}, and η represents the nitrogen oxide radical-scavenging rates in percentage. The corresponding parameters are shown in Table 3.

The values of 50% inhibitory concentration (IC50) and 95% confidence interval (CI) are shown in Table 4. They were analyzed and calculated by SPSS 17.0. IC50 represents the concentration of an inhibitor that is required for 50% inhibition of things. IC50 refers to the concentration of PAOP-C_{60} when 50% nitrogen oxide radicals were removed effectively,

Table 3 Fitting parameters of DPA, 2a, and 2b

Stab.	a		b		r
	Value	σ	Value	σ	
DPA	42.75	1.24	0.35	0.02	0.9995
2a	88.38	8.57	0.29	0.07	0.9924
2b	101.07	2.87	0.29	0.02	0.9993

Table 4 Nitrogen oxide radical scavenging activity of 2a and2b

Stab.	IC50 (g L^{-1})	95% CI (g L^{-1})
DPA	1.717	1.388–2.522
2a	0.818	0.645–1.025
2b	0.674	0.516–0.829

thereby directly showing the efficiency of PAOP-C_{60} in scavenging nitrogen oxide radicals. Only the lower concentration of PAOP-C_{60} was needed to achieve the half inhibition of nitrogen oxide radicals within the high CI.

The characterization of the NO_2-C_{60}-DBTMP derivatives during the thermal decomposition of nitrocellulose was shown in Fig. 10. The FTIR spectrum suggested the formation of –C_{60}–NO_2 bonds with the peaks –NO_2 peaks at 1537 cm^{-1} and 1370 cm^{-1}, and the peak C–N peak at 1266 cm^{-1}, which confirmed the aromatic nitro groups existed in the intermediate product. The results further indicated that the PAOP-C_{60} were involved in the inhibition of autocatalytic decomposition of nitrocellulose.

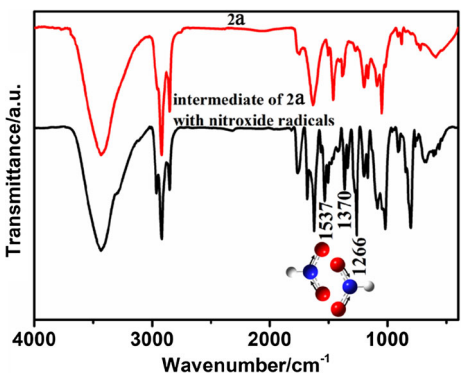

Fig. 10 FTIR spectra of the second derivative of 2a during thermal decomposition of nitrocellulose

Based on the above analysis, the stabilization mechanism of PAOP-C_{60} was proposed (Fig. 11). These fullerene derivatives have the advantage of retaining the original carbon cage structure of fullerene without destroying the chemical characteristics of fullerene. The characteristics of fullerene enable the PAOP-C_{60} to scavenge efficiently the nitrogen oxide radicals from the thermal decomposition of nitrocellulose and inhibit effectively the thermal decomposition of nitrocellulose.

Conclusion

In this investigation, the PAOP-C_{60} was synthesized and characterized via FTIR, UV–Vis and NMR. Interestingly, the all five organic addends of PAOP-C_{60} are attached to one hemisphere of the fullerene molecule around a central pentagon unit, forming a badminton-like structure, which superior in retaining the original carbon cage structure of fullerene without destroying the chemical characteristics of fullerene. The results of thermal analysis showed that the PAOP-C_{60} had good compatibility with nitrocellulose, and

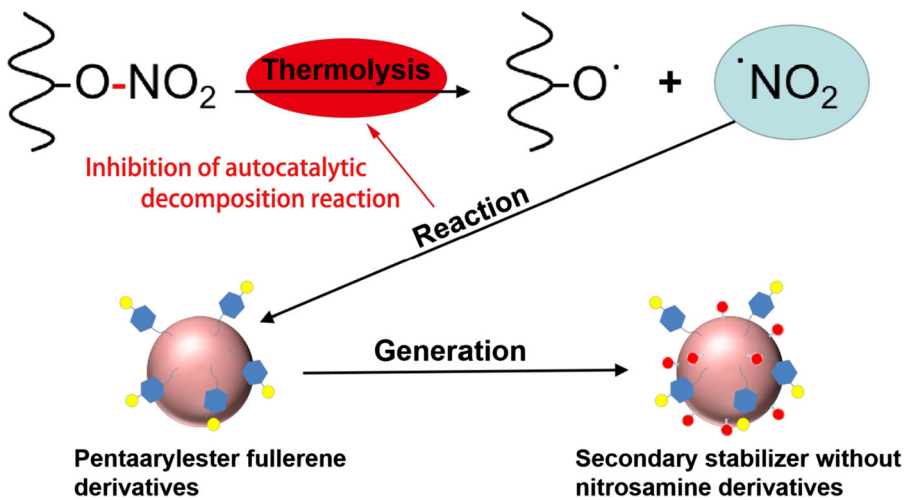

Fig. 11 Stabilization mechanism of PAOP-C_{60}

was found to exhibit superior thermal stability than traditional stabilizer DPA. The ability of PAOP-C_{60} to scavenge nitrogen oxide radicals was proved via ESR, and the intermediate product produced by PAOP-C_{60} and nitrocellulose was extracted and characterized. A possible stabilization mechanism of PAOP-C_{60} was proposed that the PAOP-C_{60} can inhibit the autocatalytic decomposition of nitrocellulose by reacting directly with the nitrogen oxide radicals produced by the thermal decomposition of nitrocellulose. Moreover, in consideration of the high carbon content and amine-free of the PAOP-C_{60}, more efforts will be made in future to investigate their potential applications in nitrocellulose-based propellant burning rate catalysis. The obtained results indicate that PAOP-C_{60} expected to be a green and efficient stabilizer for nitrocellulose, and this investigation will provide new insight into strategies for improving the safe of nitrocellulose storage.

Acknowledgments This work was supported by the financial support received from the Key Projects of the Pre-research Fund of the General Armament Department (Project No. 6140720020101), National Natural Science Foundation of China (51572230), Outstanding Youth Science and Technology Talents Program of Sichuan (No. 19JCQN0085), National Defense Technology Foundation Project (Project No. JSJL2016404B002) and the Institute of Chemical Materials, China Academy of Engineering Physics.

References

Bhattacharya A (2005) A general kinetic model framework for the interpretation of adiabatic calorimeter rate data. Chem Eng J 110:67–78

Birkett PR, Avent AG, Darwish AD, Kroto HW, Walton DRM (1993) Preparation and ^{13}C NMR spectroscopic characterisation of $C_{60}Cl_6$. J Chem Soc, Chem Commun 24:1230–1232

Birkett PR, Avent AG, Darwish AD, Hahn I, Kroto HW, Langley GJ, Loughlin JO, Taylor R, Walton DRM (1997) Arylation of [60]fullerene via electrophilic aromaticsubstitution involving the electrophile $C_{60}Cl_6$: frontside nucleophilic substitution of fullerenes. J Chem Soc Perkin Trans 2(6):1121–1126

Dong Y, Hiroshi H, Kazutoshi K (2003) Predicting the self-accelerating decomposition temperature (SADT) of organic peroxides based on non-isothermal decomposition behavior. J Loss Prev Process Ind 16:411–416

Drzyzga O (2003) Diphenylamine and derivatives in the environment: a review. Chemosphere 53:809–818

Fryš O, Bajerová P, Eisner A, Skládal J, Ventura K (2011) Utilization of new non-toxic substances as stabilizers for nitrocellulose-Based propellants. Propellants Explosives Pyrotech 36:347–355

Gharbi N, Pressac M, Hadchouel M, Szwarc H, Wilson SR, Moussa F (2005) [60]Fullerene is a powerful antioxidant in vivo with no acute or subacute toxicity. Nano Lett 5:2578–2585

Hare JP, Kroto HW, Taylor R (2013) Reprint of: preparation and UV/visible spectra of fullerenes C_{60} and C_{70}. Chem Phys Lett 589:57–60

Hassan MA, Shehata AB (2010) Studies on some acrylamido polymers and copolymer as stabilizers for nitrocellulose. J Appl Polym Sci 85:2808–2819

He Y, Liu J, Li P, Chen M, Wei R, Wang J (2017) Experimental study on the thermal decomposition and combustion characteristics of nitrocellulose with different alcohol humectants. J Hazard Mater 340:202–210

Heil M, Kerstin W, Manfred AB (2017) Characterization of gun propellants by Longmilerm mass loss measurements. Propellants Explosives Pyrotech 42:706–711

Hussien AE, Elbeih A, Klapötke TM, Krumm B (2018) Higher performance and safer handling: new formulation based on 2,2,2-trinitroethyl-formate and nitrocellulose. ChemPlusChem 83:128–131

Jain S, Park W, Chen YP, Qiao L (2016) Flame speed enhancement of a nitrocellulose monopropellant using graphene microstructures. J Appl Phys 120:370–418

Katoh K, Yoshino S, Kubota S, Wada Y, Ogata Y, Nakahama M, Kawaguchi S, Arai M (2010) The effects of conventional stabilizers and phenol compounds used as antioxidants on the stabilization of nitrocellulose. Propellants Explosives Pyrotech 32:314–321

Klerk D, Wim PC (2015) Assessment of stability of propellants and safe lifetimes. Propellants Explosives Pyrotech 40:388–393

Krumlinde P, Tunestål SEE, Hafstrand A (2016) Synthesis and characterization of novel stabilizers for nitrocellulose-based propellants. Propellants Explosives Pyrotech 42:78–83

Krusic PJ, Wasserman E, Keizer PN, Morton JR, Preston KF (1991) Radical Reactions of C60. Science 254:1183–1185

Kubota N (2010) Role of additives in combustion waves and effect on stable combustion limit of double-base propellants. Propellants Explosives Pyrotech 3:163–168

Lindblom T (2002) Reactions in stabilizer and between stabilizer and nitrocellulose in propellants. Propellants Explosives Pyrotech 27:197–208

Luo LQ, Jin B, Chai ZH, Huang Q, Chu SJ, Peng RF (2019a) Interaction and mechanism of nitrocellulose and *N*-methyl-4-nitroaniline by isothermal decomposition method. Cellulose 26:9021–9033

Luo LQ, Jin B, Xiao YY, Zhang QC, Chai ZH, Huang Q, Chu SJ, Peng RF (2019b) Study on the isothermal decomposition kinetics and mechanism of nitrocellulose. Polym Test 75:337–343

Merzhanov AG, Abramov VG (2010) Thermal explosion of explosives and propellants. Propellants Explosives Pyrotech 6:130–148

Morley D, Keefer LK (1993) Nitric oxide/nucleophile complexes: a unique class of nitric oxide-based vasodilators. J Cardiovasc Pharmacol 22:3–9

Ossa M, López-López M, Torre M, García-Ruiz C (2011) Analytical techniques in the study of highly-nitrated nitrocellulose. TrAC Trends Anal Chem 30:1740–1755

Purves CB, Grassie VR, Mitchell L, Pepper JM (1950) Preliminary tests on possible new stabilizers for nitrocelluloses. Can J Res 28:468–484

Saunders CW, Taylor LT (1990) A review of the synthesis, chemistry and analysis of nitrocellulose. J Energ Mater 8:149–203

Tang Q, Fan X, Li J, Bi F, Fu X, Zhai L (2016) Experimental and theoretical studies on stability of new stabilizers for *N*-methyl-P-nitroaniline derivative in CMDB propellants. J Hazard Mater 327:187–196

Taylor R, Walton DRM (1993) The chemistry of fullerenes. Nature 363:685–693

Trache D, Tarchoun AF (2018) Stabilizers for nitrate ester-based energetic materials and their mechanism of action: a state-of-the-art review. J Mater Sci 53:100–123

Tsang W, Herron JT (1991) Chemical kinetic data base for propellant combustion I. reactions involving NO, NO_2, HNO, HNO_2, HCN and N_2O. J Phys Chem Ref Data 20:609–663

Wang B, Xin L, Wang Z, Deluca LT, Liu Z, You F (2017) Preparation and properties of a nRDX-based propellant. Propellants Explosives Pyrotech 42:649–658

Wiegand DA, Nicolaides S, Pinto J (1990) Mechanical and thermomechanical properties of NC base propellants. J Energ Mater 8:442–461

Wilker S, Heeb G, Vogelsanger B, Petržílek J, Skládal J (2007) Triphenylamine-a 'New' stabilizer for nitrocellulose based propellants-part I: chemical stability studies. Propellants Explosives Pyrotech 32:135–148